

Electronic Supplementary Information

Multicolor vision perception of flexible optoelectronic synapse with high-sensitivity for skin sunburn warning

Yaqian Yang,^{1,2} Ying Li,^{*1} Di Chen,^{1,2} Guozhen Shen^{*1}

Dr. Yaqian Yang, Dr. Ying Li, Prof. Di Chen, Prof. Guozhen Shen
School of Integrated Circuits and Electronics
Beijing Institute of Technology
Beijing 100081, China
E-mail: liying0326@bit.edu.cn; gzshen@bit.edu.cn

Dr. Yaqian Yang, Prof. Di Chen
School of Mathematics and Physics
University of Science and Technology Beijing
Beijing 100083, China.

Keywords: lead-free halide perovskite, flexible artificial synapse, multicolor vision perception, high-sensitivity, skin sunburn warning

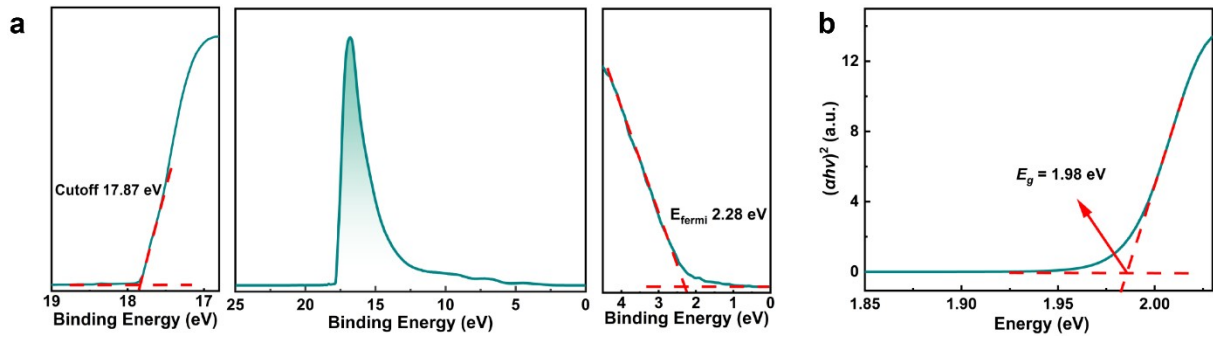


Fig. S1 (a) UPS data of the PEA₂SnI₄ films. (b) Tauc plot of the PEA₂SnI₄ film.

The work function was calculated using the following formulas:¹

$$E_F = -21.22 + E_{\text{cutoff}} \quad (1)$$

in which E_{cutoff} is the binding energy of the second-order cutoff in the spectrum. It can be calculated as -3.35 eV. E_{Fermi} is the difference between the Fermi energy and the E_{VBM} . Thus, the calculated value of E_{VBM} is 5.63 eV. The Tauc plot reveals that the direct band gap (E_g) of the Cs₃Bi₂Br₉ film to be 1.98 eV. Therefore, on the basis of E_{VBM} and E_g ($E_g = E_{\text{CBM}} - E_{\text{VBM}}$), the conduction band (E_{CBM}) can be calculated as -3.65 eV.

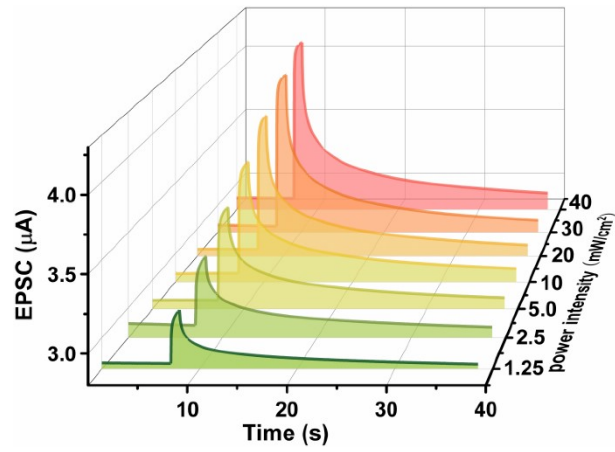


Fig. S2 EPSC behavior triggered by illumination for 1 s at different optical power densities (520 nm, 3 V, pulse width of 1 s).

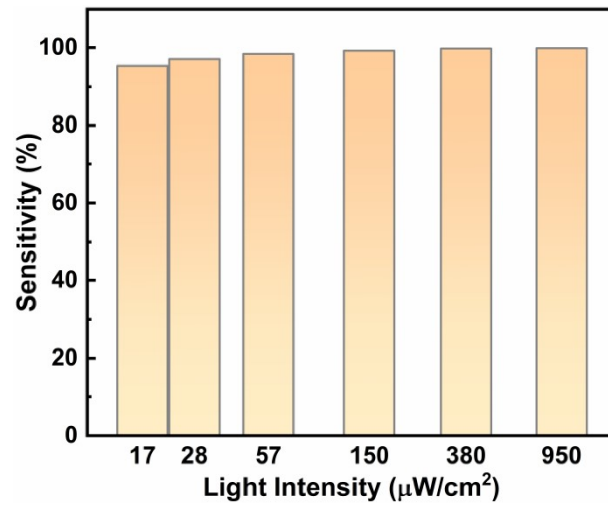


Fig. S3 *S* versus light intensity of PEA₂SnI₄/ZnO devices under weak light illumination.

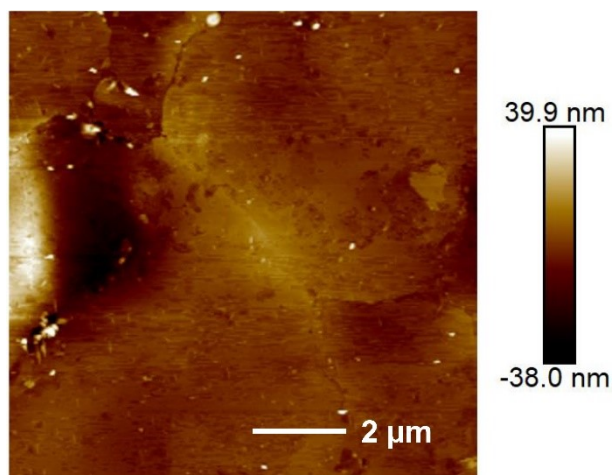


Fig. S4 AFM images of PEA₂SnI₄ film.

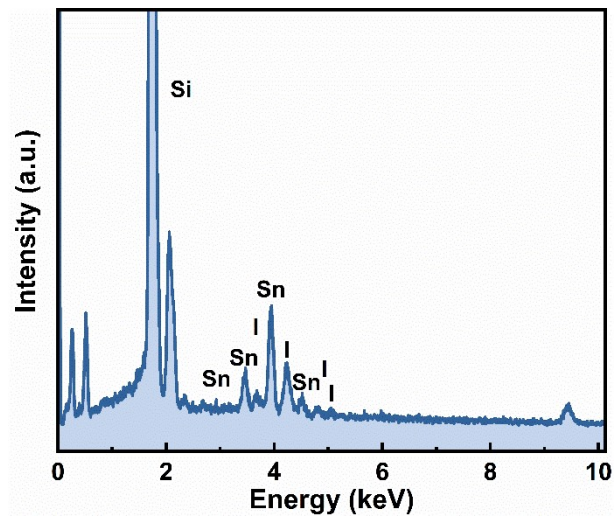


Fig. S5 EDS spectra of the PEA_2SnI_4 films.

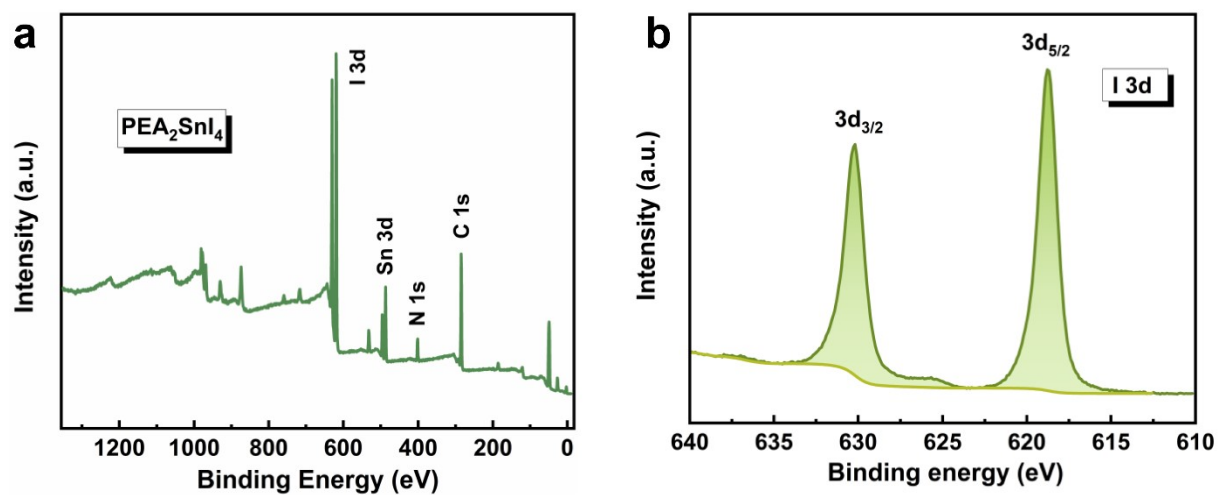


Fig. S6 (a) XPS spectra of PEA₂SnI₄ films and the high-resolution spectra of (b) I 3d.

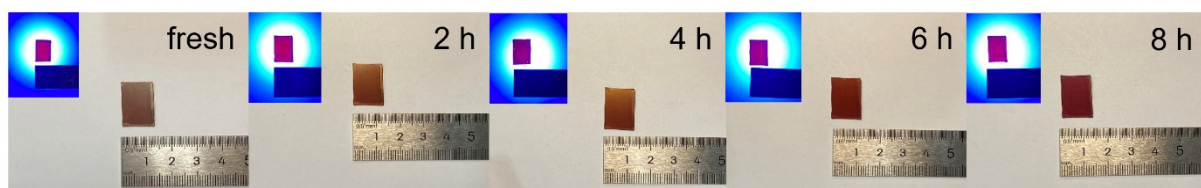


Fig. S7 The optical photographs of the PEA₂SnI₄ films after different storage periods under air conditions.

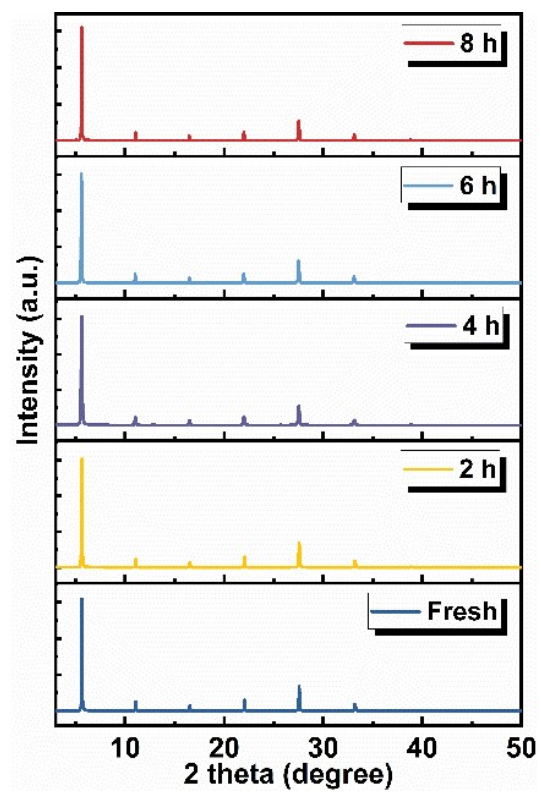


Fig. S8 XRD measurements of the PEA₂SnI₄ films after different storage periods under air conditions.

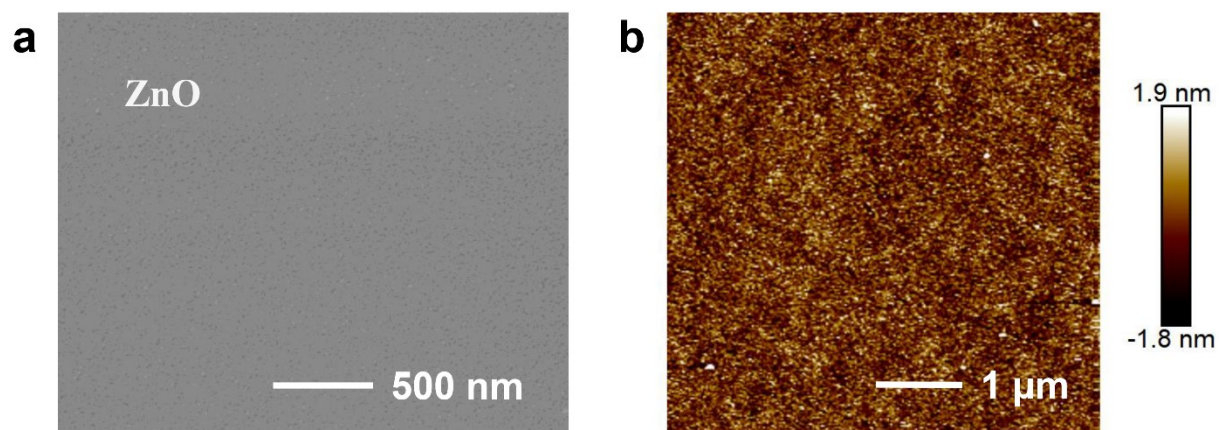


Fig. S9 (a) Top-view SEM image of ZnO film and (b) corresponding AFM images.

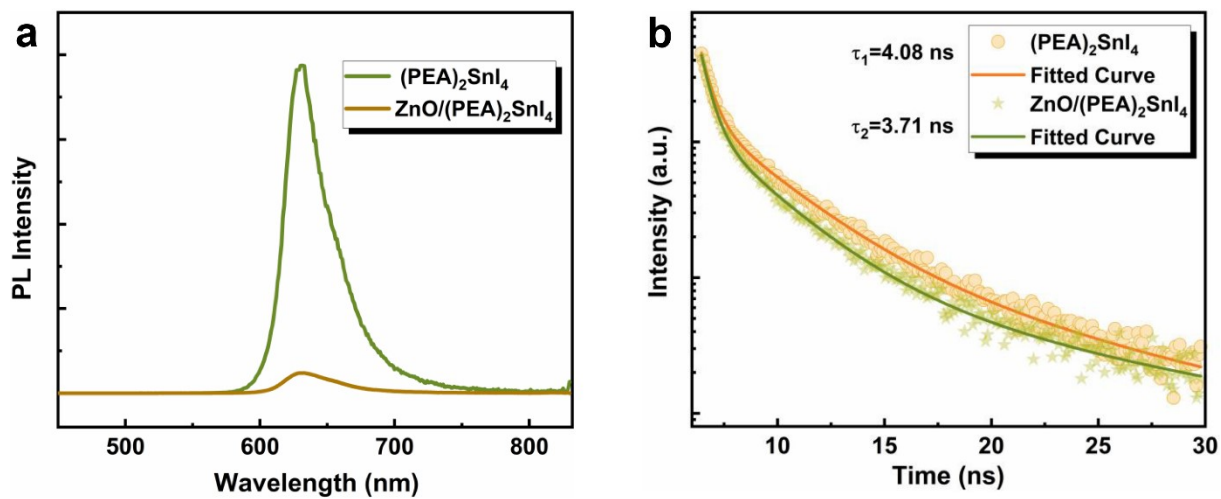


Fig. S10 (a) PL spectra and (b) the time-resolved PL decay and fitting curves of $(\text{PEA})_2\text{SnI}_4$ and the $(\text{PEA})_2\text{SnI}_4/\text{ZnO}$ films.

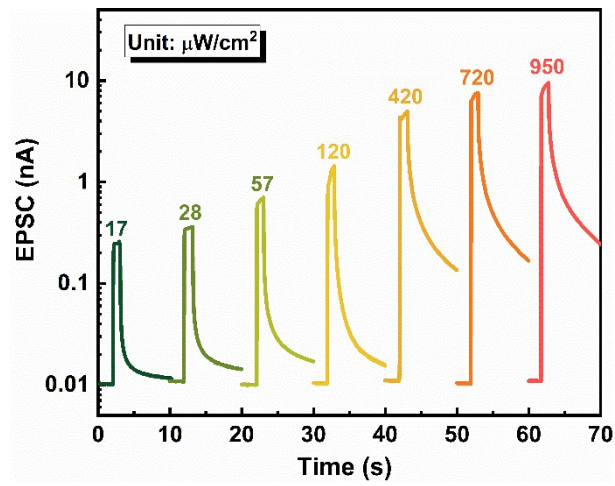


Fig. S11 EPSC behavior triggered by illumination for 1 s at weak optical power densities (520 nm, 0 V, pulse width of 1 s).

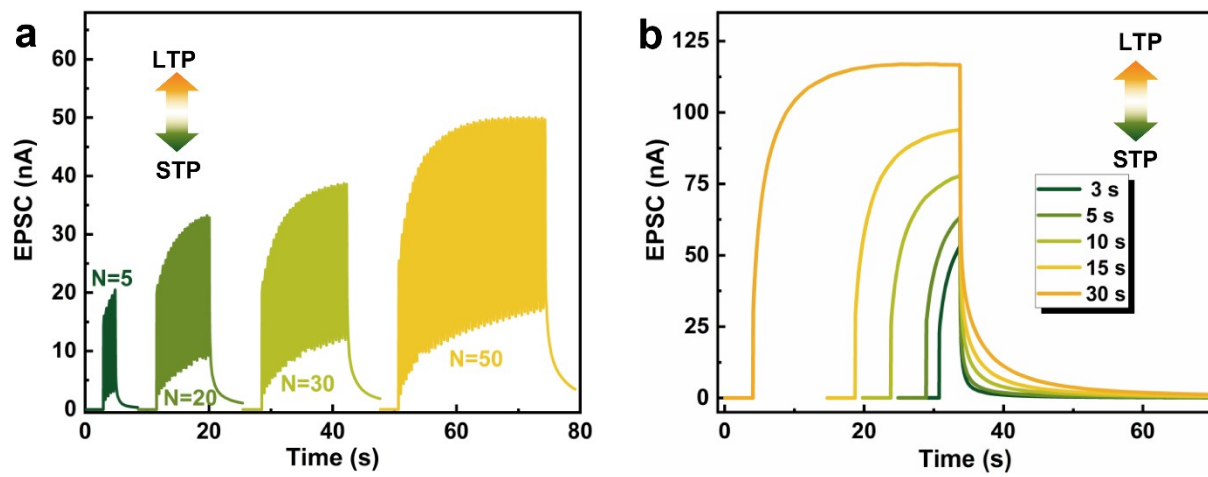


Fig. S12 The EPSC behavior of the device measured at (a) different pulse numbers and (b) different illumination time.

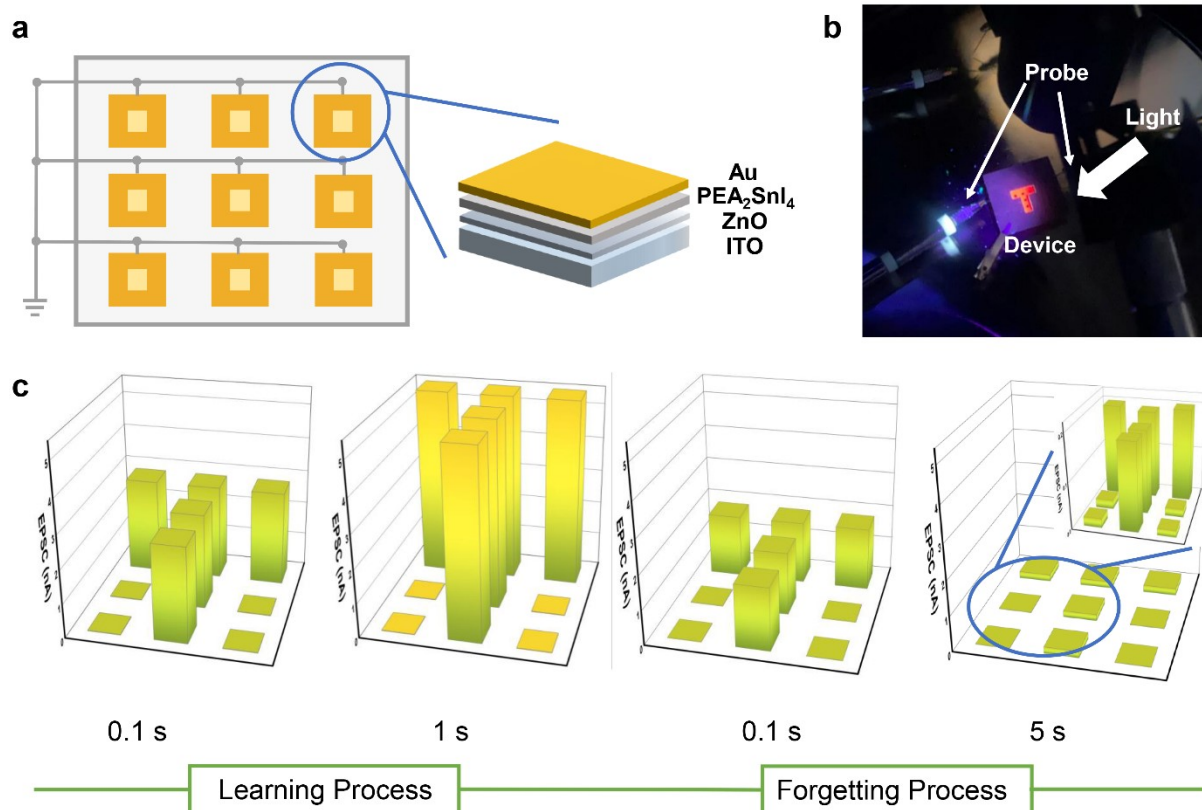


Fig. S13 (a) Schematic diagram of a 3×3 synaptic device arrays. (b) Optical photographs of the test. (c) Visualization of the learning and forgetting curve of the letter “T” (520 nm, 420 μW cm⁻²).

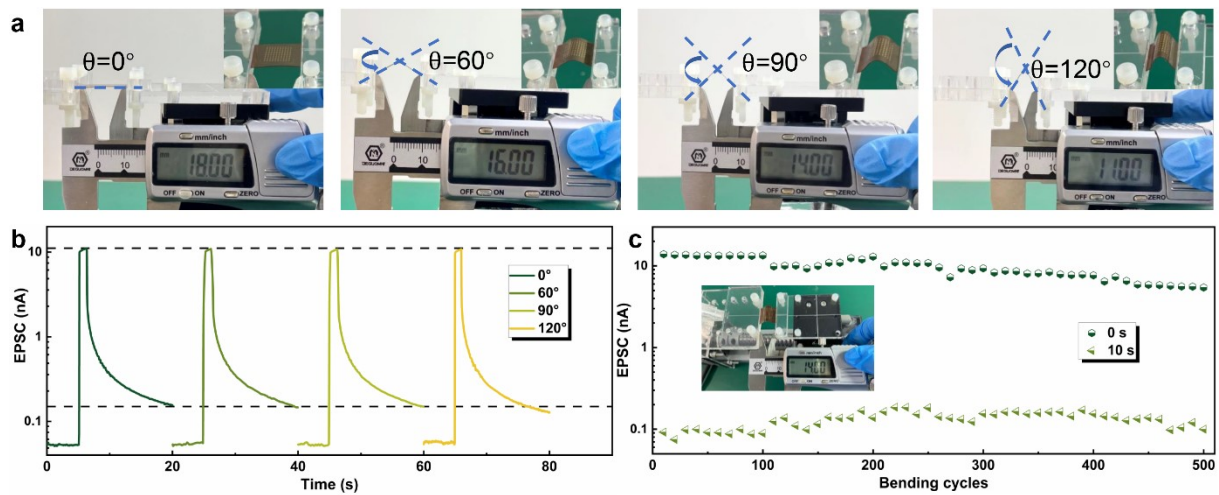


Fig. S14 (a) Optical images at different bending angles and (b) corresponding EPSC after 1 s of illumination. (c) Changes in EPSC values when light is withdrawn for 0 and 10 seconds (exposure for one second under $520\text{ nm}, 1.25\text{ mW cm}^{-2}$). The bending cycles are 500 cycles with an interval of 10 cycles.

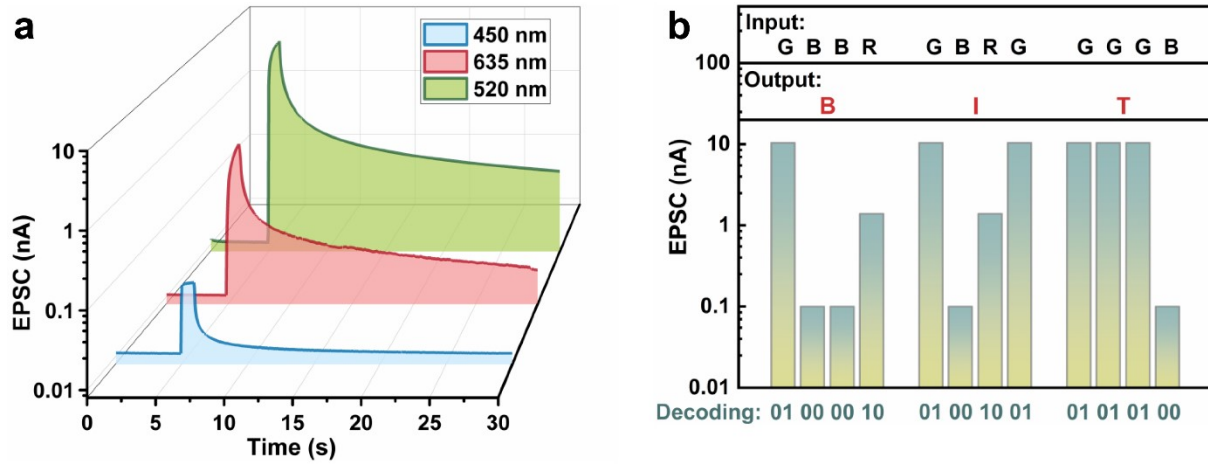


Fig. S15 (a) EPSC behavior triggered by light of different wavelength with the same pulse width (1 s, 450 nm 420 uW cm^{-2} , 520 nm 1.25 mW cm^{-2} , 635 nm, 420 uW cm^{-2}). (b) The decode results of the photoelectronic synapse to the American Standard Code for Information Interchange (ASCII).



Fig. S16 Photographs for optical displays of the designed flexible circuit board on a (a) canvas bag and (b) hat.

Table S1 Comparisons between previous low-energy synaptic devices and this work.

Device Structure	P ($\mu\text{W cm}^{-2}$)	λ (nm)	Opt. Volt (V)	ΔE (J)	S (%)	Ref
PEA₂SnI₄/ZnO	17	520	0	0	95.38	This work
Al ₂ O ₃ /CdS	2.48×10 ³	365	—	0	20.00	[2]
DPPDTT/CsPbBr ₃ QD	50	450	-0.5 m	25 f	20	[3]
BP flakes	2×10 ³	280	50 m	5.75 n	26.09	[4]
2DP/PMMA/pentacene	690	400	0.1	0.29 p	33.3	[5]
ReS ₂ /h-BN/monographene	0.11 nW/ μm^2	532	0.1	0.06 n	41.67	[6]
Dif-TES-ADT	—	—	0.1	0.07~34 f	50	[7]
ZnO/MoO ₃ /Mo	8	390	—	37 p	66.67	[8]
CNT/CsPbBr ₃ QD	48	516	5	1.7 n	70.59	[9]
Ag/BiOI/Pt	—	400	0.01	100 f	75	[10]
CsPbBr ₃ /PDPP4T	650	450	10 μ	1.3 f	98.33	[11]
CsBi ₃ I ₁₀ /PDPP4T	320	430	-1	1.25 n	99.2	[12]

References

- 1 Y. J. Liu, Y. X. Gao, J. Y. Zhi, R. Q. Huang, W. J. Li, X. Y. Huang, G. H. Yan, Z. Ji and W. J. Mai, *Nano Res.*, 2022, **15**, 1094.
- 2 X. Han, Y. Zhang, Z. Huo, X. Wang, G. Hu, Z. Xu, H. Lu, Q. Lu, X. Sun, L. Qiu, P. Yan and C. Pan, *Adv. Electron. Mater.*, 2023, **9**, 2201068.
- 3 D. Hao, J. Zhang, S. Dai, J. Zhang and J. Huang, *ACS Appl. Mater. Interfaces*, 2020, **12**, 39487.
- 4 T. Ahmed, M. Tahir, M. X. Low, Y. Ren, S. A. Tawfik, E. L. H. Mayes, S. Kuriakose, S. Nawaz, M. J. S. Spencer, H. Chen, M. Bhaskaran, S. Sriram and S. Walia, *Adv. Mater.*, 2021, **33**, e2004207.
- 5 J. Zhang, Q. Shi, R. Wang, X. Zhang, L. Li, J. Zhang, L. Tian, L. Xiong and J. Huang, *InfoMat*, 2021, **3**, 904.
- 6 Y. Chen, Y. Kang, H. Hao, X. Xie, J. Zeng, T. Xu, C. Li, Y. Tan and L. Fang, *Adv. Funct. Mater.*, 2022, **33**, 2209781.
- 7 J. Shi, J. Jie, W. Deng, G. Luo, X. Fang, Y. Xiao, Y. Zhang, X. Zhang and X. Zhang, *Adv. Mater.*, 2022, **34**, e2200380.
- 8 T. Guo, B. Zhang, X. Wang, Y. Xiao, B. Sun, Y. N. Zhou and Y. A. Wu, *Adv. Funct. Mater.*, 2023, **33**, 2303879.
- 9 Q. B. Zhu, B. Li, D. D. Yang, C. Liu, S. Feng, M. L. Chen, Y. Sun, Y. N. Tian, X. Su, X. M. Wang, S. Qiu, Q. W. Li, X. M. Li, H. B. Zeng, H. M. Cheng and D. M. Sun, *Nat. Commun.*, 2021, **12**, 1798.
- 10 P. Lei, H. Duan, L. Qin, X. Wei, R. Tao, Z. Wang, F. Guo, M. Song, W. Jie and J. Hao, *Adv. Funct. Mater.*, 2022, **32**, 2201276.
- 11 T. Chen, X. Wang, D. Hao, S. Dai, Q. Ou, J. Zhang and J. Huang, *Adv. Optical Mater.*, 2021, **9**, 2002030.
- 12 R. Wang, P. Chen, D. Hao, J. Zhang, Q. Shi, D. Liu, L. Li, L. Xiong, J. Zhou and J. Huang, *ACS Appl. Mater. Interfaces*, 2021, **13**, 43144.